This material is posted here with permission of the IEEE. Such permission of the IEEE does not in any way imply IEEE endorsement of any of Helsinki University of Technology's products or services. Internal or personal use of this material is permitted. However, permission to reprint/republish this material for advertising or promotional purposes or for creating new collective works for resale or redistribution must be obtained from the IEEE by writing to pubs-permissions@ieee.org.

By choosing to view this document, you agree to all provisions of the copyright laws protecting it.

Publication [P3]

O. Kivekäs, J. Ollikainen, T. Lehtiniemi, and P. Vainikainen, “Bandwidth, *SAR*, and efficiency of internal mobile phone antennas,” *IEEE Transactions on Electromagnetic Compatibility*, vol. 46, no. 1, Feb. 2004, pp. 71-86. © 2004 IEEE. Reprinted with permission.

Bandwidth, SAR, and Efficiency of Internal Mobile Phone Antennas

Outi Kivekäs, Jani Ollikainen, *Member, IEEE*, Tuukka Lehtiniemi, and Pertti Vainikainen, *Member, IEEE*

***Abstract*—This paper presents a thorough investigation into the effects of several phone chassis-related parameters—length, width, thickness, and distance between the head and phone—on the bandwidth, efficiency, and specific absorption rate (SAR) characteristics of internal mobile phone antennas. The studied antenna-chassis combinations are located beside an anatomical head model in a position of actual handset use. The effect of the user's hand is also studied with two different hand models. The main part of the study is based on FDTD simulations, but also experimental results, which support the computationally obtained conclusions, are given. The presented analysis provides novel and useful information for future design of mobile handset antennas. The results show the general trends of bandwidth, SAR, and efficiency with different chassis parameters. The results also reveal a connection between these three performance parameters: an increase in SARs and a decrease in radiation efficiency occur compared to the general trend when the bandwidth reaches its maximum. This happens when the resonant frequency of the chassis equals that of the antenna.**

***Index Terms*—Bandwidth, efficiency, handset antennas, mobile communications, specific absorption rate (SAR).**

I. Introduction

THE ELECTRICAL characteristics of a mobile handset antenna depend strongly on the size of the ground plane of the device on which the antenna is mounted (phone chassis, which typically consists of the printed circuit board and the RF shield) and the position of the antenna on it [1]–[4]. As the combined behavior of antenna element and phone chassis determines the performance, the chassis dimensions are an essential part of handset antenna design.

Previous research has focused on the effect of the length of the metal chassis of a handset on bandwidth [1]–[8]. The results indicate that the total radiation bandwidth of the antenna-chassis combination is partly defined by the dipole-type radiation of the chassis currents, whose level further depends on whether the chassis is at resonance or not [4], [5]. If the chassis resonates at the operating frequency of the antenna element, the bandwidth of the antenna-chassis combination increases strongly. When the chassis resonance is farther from the operating frequency, the bandwidth decreases due to the smaller contribution of the chassis. In general, the contributions of the antenna element and phone chassis to the radiation bandwidth depend on the design and operating frequency of the structure.

Besides the bandwidth, another important consideration of handset antenna design involves the interaction of electromagnetic radiation with human body, which has been widely investigated, e.g., in [9], [10]. However, concerning the effect of the phone chassis, the results are limited. Based on the bandwidth studies, it nevertheless can be expected that the effect of the chassis is significant also from the handset-user interaction point of view. Only few investigations have been published relating to this issue [8],[11]. These two studies present some results on the specific absorption rate (SAR) behavior of handset antennas with different chassis dimensions positioned beside simplified head models. However, a systematic characterization and analysis of the chassis effect on antenna performance has not previously been carried out. Furthermore, the topic has not been studied with an anatomical head model so far; neither the effect of the user's hand with different chassis parameters has been published. In addition, the behavior of radiation efficiency as functions of chassis dimensions has not been investigated before.

The purpose of this paper is first to demonstrate that it is essential to identify the significance of different parts of antenna-chassis combination on mobile-phone antenna performance, and further to demonstrate the general trends of bandwidth, SAR, and efficiency with different chassis parameters. The paper presents a comprehensive study for two coarse phone models, which comprise an internal patch antenna and phone chassis, and are positioned beside an anatomical head model. One of the phones is for 900 MHz and the other for 1800 MHz. The approach is based on the modal analysis [4] with a basic idea that an antenna-chassis combination supports two significant, fairly independent wavemodes: the compact quasi-TEM wavemode of a self-resonant antenna element and the single-wire waveguide-type wavemode of a chassis resembling a thick dipole. The main part of the study is based on simulations, but the applicability of the simulation models is confirmed by a comparison with measured results. The effect of the chassis length on the bandwidth, efficiency, and SAR characteristics of handset antenna-chassis combinations is presented and analyzed first, including an investigation with two different hand models. This is followed by an analysis of the effect of other chassis-related parameters: chassis width, thickness, distance between the head and phone, and hand position. The last part of the paper is devoted to a discussion on

Manuscript received January 8, 2003; revised July 2, 2003. This work was supported in part by the Academy of Finland, in part by Graduate School in Electronics, Telecommunications, and Automation (GETA), in part by the Finnish Society of Electronics Engineers, in part by Emil Aaltonen Foundation, in part by Ulla Tuominen Foundation, and in part by Nokia Foundation.

O. Kivekäs, T. Lehtiniemi, and P. Vainikainen are with the Institute of Digital Communications, SMARAD/Radio Laboratory, Helsinki University of Technology, Espoo FIN-02015, Finland (e-mail: outi.kivekas@hut.fi; tlehtini@cc.hut.fi; pertti.vainikainen@hut.fi).

J. Ollikainen is with the Nokia Research Center, Radio Communications Laboratory, Helsinki FIN-00045, Finland (e-mail: jani.ollikainen@nokia.com).

Digital Object Identifier 10.1109/TEMC.2004.823613

0018-9375/04$20.00 © 2004 IEEE

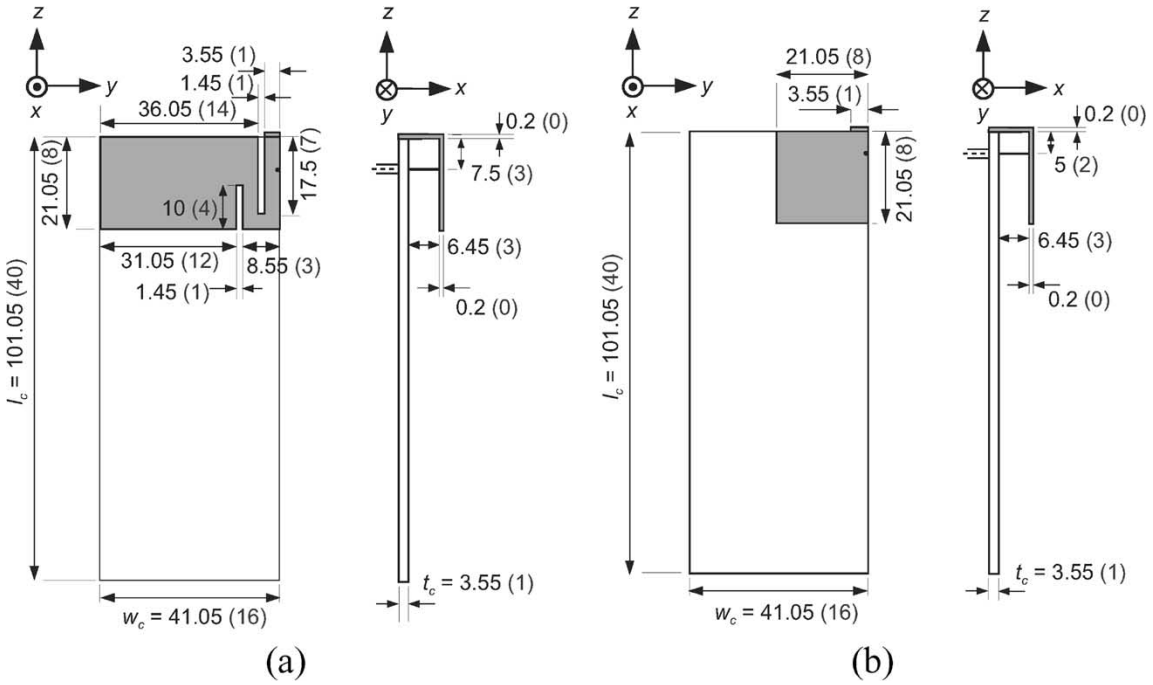

Fig. 1. Phone models with internal patch antennas for (a) 900 and (b) 1800 MHz. Dimensions outside parentheses are in millimeters and dimensions in parentheses are given as numbers of FDTD cells.

the results and on their implications for mobile-phone antenna design applications.

II. Simulation Methods and Models

A. General

A finite-difference time-domain (FDTD) based commercial electromagnetic solver (XFDTD, Ver. 5.1 Bio-Pro) was used for the most part of the study. Unless otherwise stated, the presented results are based on FDTD simulations. The used cell size was $\Delta x = \Delta y = \Delta z = 2.5$ mm. The total size of the simulation space, including head and hand models, was $195 \times 150 \times 168$ cells $(x \times y \times z)$. Second-order stabilized Liao boundaries were used as absorbing boundary conditions. The antennas were excited with a gap voltage source with a 50-Ω series source resistance for decreasing the number of timesteps required for convergence [12]. Transient excitation using a Gaussian derivative pulse was used in the bandwidth calculations. The SARs and radiation efficiencies were calculated at 900 and 1800 MHz using a sinusoidal excitation. The simulations were run for 4000 time steps with $\Delta t = 4.815$ ps to obtain the convergence or steady-state condition. All presented SAR values are normalized to 1 W of continuous wave (CW) input power. However, it must be noted that the specified mean antenna input powers for handsets e.g., in GSM900, GSM1800, and UMTS systems are 250, 125, and 250 mW, respectively. Both 1- and 10-g average SARs are given owing to their use in different regulations.

Besides the FDTD method, a method-of-moments (MoM) based commercial full-wave electromagnetic simulator (IE3D, Ver. 5.2) was used to study the bandwidth performances of the structures in free space. It was used for more accurate evaluation of the bandwidths of the prototypes, because the simulated impedance results obtained with the software have previously been shown to agree very well with the experimental ones for similar antenna-chassis structures [13], and because such detailed antenna modeling could not be done with the FDTD method (see Section II-B).

B. Antenna and Phone Models

Two shorted patch antennas, one for 900 MHz and the other for 1800 MHz, were designed for the study (Fig. 1). They represent typical modern internal mobile phone antennas. The antennas were designed with the FDTD method, where the voxel size of the head model ($\Delta x = \Delta y = \Delta z = 2.5$ mm) restricted the description accuracy of the antennas. When the dimensions were transformed from FDTD cells into millimeters for the MoM simulations and prototyping, the effective radius of a wire consisting of one metal FDTD cell edge was taken into account using the value $0.21\Delta x$ based on [14], except in the thickness of the antenna element plate and short circuit. Because of this, the dimensions of the structures are not multiples of 2.5 mm. Furthermore, the feed probe (diameter 0.5 mm) was modeled using the thin-wire approximation of XFDTD. The location of the feed probe was kept constant for all the studied configurations. A simple metal plate modeled the phone chassis in the simulations. The chassis dimensions in the design phase were roughly 101 mm $\times$ 41 mm $\times$ 3.6 mm (length $\times$ width $\times$ thickness, $l_c \times w_c \times t_c$), representing the typical dimensions of a modern mobile handset chassis.

C. Head Model

An anatomical head model consisting of six tissue types was selected for the simulation study for realistic human head modeling. The used head model was an FDTD mesh with 2.5 mm voxel resolution remeshed from a standard anatomical human head and shoulders model (voxel size 3 mm), obtained from the

TABLE I
VALUES OF TISSUE PARAMETERS (RELATIVE PERMITTIVITY ϵ_r', EFFECTIVE CONDUCTIVITY σ, DENSITY ρ)

Tissue	900 MHz		1800 MHz		
	ε_r'	σ (S/m)	ε_r'	σ (S/m)	ρ (kg/m^3)
Cartilage	42.65	0.782	40.21	1.287	1100
Muscle	55.95	0.969	54.44	1.389	1050
Eye	55.27	1.167	53.57	1.602	1020
Brain	45.80	0.766	43.54	1.153	1040
Dry skin	41.40	0.867	38.87	1.184	1090
Skull (Bone)	16.62	0.242	15.56	0.432	1645

software provider. The values of the relative permittivity ϵ_r' and effective conductivity σ of the tissues were interpolated in frequency-domain from the values given in [15]. The tissue densities (ρ) were obtained from [16] and [17]. All the used tissue parameters are given in Table I.

The phone models were positioned beside the head according to the intended use position specified by CENELEC [18]. Relative to the head, the phone was tilted 74° from vertical and 10° from the ear toward the cheek, as described in [19]. To avoid staircasing errors in the phone, it was kept aligned with the original axes of the coordinate system (Fig. 1) while the head was rotated. In most cases a distance of $d \approx 7$ mm (3 cells) was left between the head and the back side of the phone chassis, as that is considered to represent the typical distance between the user's head and the metal chassis of a modern mobile handset. Some simulations were also repeated with a smaller distance $d \approx 2$ mm (1 cell), and the effect of the distance between the head and phone was studied as well.

D. Hand Models

As a hand is always present in a typical operating situation of a mobile phone, two different block models of the hand holding the handset were included in the studies (Fig. 2). The first one (hand1) was similar to a typical hand model used in the literature [10], [19]. The second model (hand2), developed in this work, simulated a more realistic way in which a small handset is held. Both models consisted of two tissues, bone surrounded by muscle. Hand1 modeled mainly the palm, while the fingers were very short [Fig. 2(a)]. The model was symmetric, i.e., the short fingers wrapped both the chassis edges similarly, and the shape of the model was identical in all xy cuts. Hand1 represented a worst case approximation, as it was detached from the metal chassis by only 2 mm. The palm of hand2 was identical to that of hand1 but here the fingers were clearly longer, thus detaching the palm from the chassis by 49.5 mm [Fig. 2(b)]. The thumb held one edge of the chassis and the rest fingers the other within a distance of 2 mm. The distance between the lower edge of the antenna element and the upper edge of both hand models was 9.5 mm. The locations of the hands were fixed with respect to the antenna element regardless of the chassis dimensions.

III. MEASUREMENT METHODS

A. General

Impedance, SAR, and efficiency measurements were carried out to validate the results obtained by simulations. Three prototypes for both frequencies were constructed with chassis lengths 61, 101, and 141 mm (chassis width $w_c = 41$ mm, chassis thickness $t_c = 3.6$ mm). The prototypes were constructed by photoetching the patch and contact pins (feed and short circuit) from 0.2 mm-thick sheet of tin bronze (96% copper and 4% tin). The phone bodies were modeled by 3.6 mm-thick aluminum boxes.

Due to practical reasons, the measurements were performed with homogeneous phantoms instead of the heterogeneous phantom used in the simulations. However, it was first studied with simulations that the general bandwidth, SAR, and efficiency characteristics as a function of chassis length with a homogeneous phantom are similar to those with the heterogeneous one. In these simulations, the shape of the head was the same as that of the heterogeneous model (see Section II-C), but the material parameters were replaced by those of the tissue-simulating liquids used in the measurements.

B. SAR

The SAR distributions were determined by measuring the electric fields inside a phantom filled with brain-simulating liquid and calculating the corresponding SAR values according to equation $\text{SAR} = \sigma \cdot |E\rightarrow|^2/\rho$. A computer-controlled three-dimensional (3-D) stepper motor system was used for positioning an isotropic E-field probe [ET3DV5R from Schmid & Partner Engineering Ag (SPEAG)] inside the phantom. At first, the probe scanned coarsely over a large volume inside the phantom to localize the maximum SAR areas. Then, the sampling was done with a finer grid around these maximum values. The Generic Twin Phantom v3.0 from SPEAG was used in the study, and the brain-simulating liquids were prepared by following the recipes given in [20] ($\epsilon_r' = 42.5$ and $\sigma = 0.85$ S/m at 900 MHz, $\epsilon_r' = 41$ and $\sigma = 1.65$ S/m at 1800 MHz). The nonmeasurable data near the phantom surface was extrapolated by fitting a second order polynomial obtained by using the least mean-square error method to the measured data, as in [21]. More data points were interpolated between the measured values using cubic spline interpolation algorithm. The volume-averaged spatial peak SAR values were derived by shifting a cube with side length of either 10 mm (1 g) or 21.5 mm (10 g) over the phantom region, and calculating the SAR averaged over each cube.

C. Radiation Efficiency

The radiation efficiencies ($\eta_r = P_{\text{rad}}/P_{\text{in}}$, do not include losses due to mismatch) of the prototypes were measured with the 3-D pattern integration method [22]. The used head model was the Generic Head Phantom v3.5 from SPEAG.

IV. DEPENDENCE OF ANTENNA PERFORMANCE ON CHASSIS LENGTH

A. Bandwidth

The effect of the chassis length on the impedance bandwidth was studied for both models of Fig. 1. The chassis length was increased so that the upper edge of the chassis and the antenna element were fixed and the lower part of the chassis was extended starting from a plate with the length equal to that of the antenna element (21 mm). The bandwidth simulations as well as

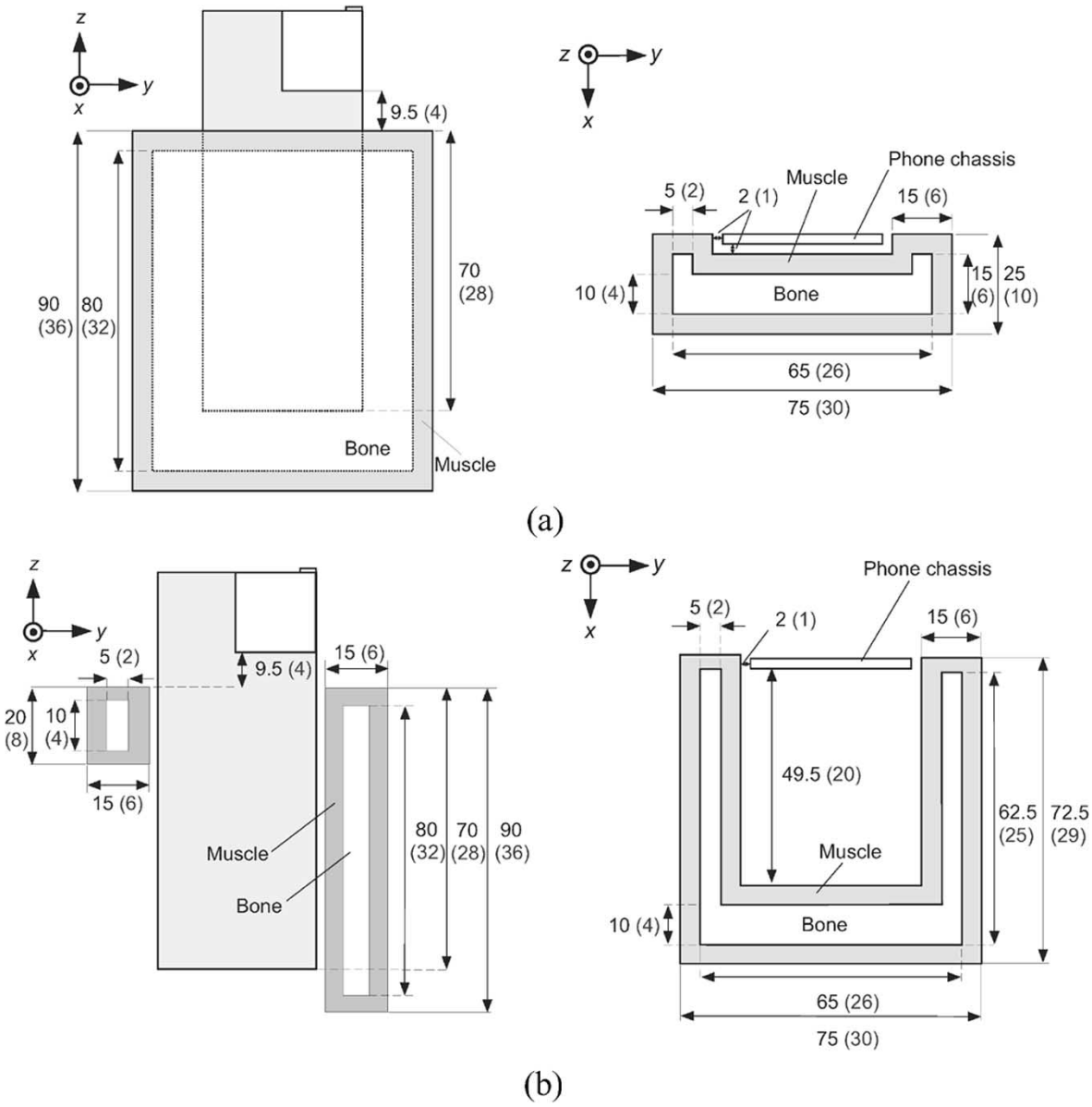

Fig. 2. Hand models used in simulations (a) hand1 (b) hand2. Dimensions outside parentheses are in millimeters, and dimensions in parentheses are given as numbers of FDTD cells. Tissue parameters for muscle and bone are given in Table I.

measurements were performed when the phones were located in free space and beside the head $(d \approx 7$ mm$)$.

The bandwidth of a resonant antenna depends on the coupling of the feed line to the antenna element, whereas the unloaded quality factor (Q_0) does not. Changing the chassis length has a considerable effect on the coupling, and thus the bandwidths in different cases were not directly comparable. In order to make the cases with different chassis lengths comparable, effective unloaded quality factors $(Q_{0,\mathrm{eff}})$ [4], which take into account the effect of the chassis, were determined for each antenna-chassis combination from their frequency responses of reflection coefficient. The relative impedance bandwidths $(L_{\mathrm{retn}} \geq 6$ dB$)$ for critically coupled (perfectly matched at resonance) antennas were then calculated from the effective unloaded quality factors using equation $B_r = (S-1)/(\sqrt{S} \cdot Q_{0,\mathrm{eff}})$[23], where S is the maximum allowed standing wave ratio (here $S = 3$).

Fig. 3 shows the simulated (MoM) impedance bandwidths in free space for the 900- and 1800-MHz antenna models as a function of the chassis length, when l_c increases from 21 to 181 mm ($w_c = 41$ mm, $t_c = 3.6$ mm). The chassis lengths were changed into wavelengths using λ_0 calculated either at 900 or at 1800 MHz, although the resonant frequencies of the antennas varied slightly as the chassis lengths were changed. Also, the measured bandwidths are shown in Fig. 3. The bandwidths are given in free space, as they are considered to represent well the typical behavior. The results showed only small changes due to the dielectric loading of the head. In addition, because of the different head models used in the simulations and measurements, it was easiest to validate the performance of the simulation models by measuring the bandwidths of the prototypes in free space. As seen in Fig. 3, a good agreement between the simulated and measured results is obtained.

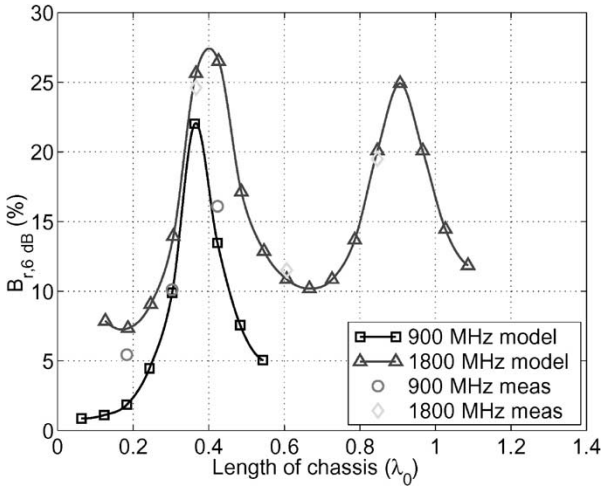

Fig. 3. Simulated (MoM) and measured impedance bandwidths ($L_{\mathrm{retn}} \geq 6$ dB) of 900- and 1800-MHz antennas in free space as a function of chassis length.

As shown in Fig. 3, the effect of the chassis length on impedance bandwidth is significant. The chassis lengths at which the bandwidth has its minimums can be assumed to represent the cases, where the contribution of the chassis radiation is small, and the bandwidth obtained is that given by the antenna element alone [4]. The increase in bandwidth is assumed to be due to the increased chassis radiation as the chassis is approaching the resonant length. For both 900- and 1800-MHz models, the bandwidth reaches its maximum when the length of the phone chassis is approximately $0.4\lambda_0$. Considering the open-end extensions of the chassis, it can be assumed that the effective length at this point is approximately $l_{c,\mathrm{eff}} = 0.5\lambda_0$, which means that at this point the chassis is resonant. This is supported by the fact that the first resonance of a simple dipole antenna occurs also when its physical length is $<0.5\lambda_0$, and as the dipole thickness increases, it must be further shortened to obtain resonance [24]. In addition, when the length of the chassis has been increased from $0.4\lambda_0$ by $0.5\lambda_0$ to $0.9\lambda_0$, there is another resonance at 1800 MHz. Such a resonance could also be expected in the case of the 900 MHz model if the chassis length was increased by the same amount in wavelengths. These results and those in [4], [5], and [7] indicate that the total bandwidth of the antenna-chassis combination is largely defined by the dipole-type chassis wavemode. It is also worth noting that the slopes of the curves of Fig. 3 are very steep near the chassis resonances. Thus, even a small change in the chassis length could affect the bandwidth significantly.

B. SAR and Radiation Efficiency

1) Without Hand: Fig. 4 shows the simulated SARs and radiation efficiencies as a function of the chassis length ($l_c =$ 21–181 mm, $w_c = 41$ mm, $t_c = 3.6$ mm) at 900 and 1800 MHz when the phones are located beside the anatomical heterogeneous head model. The results are for two distances between the head and chassis (solid lines: $d \approx 7$ mm, and dashed lines $d \approx 2$ mm).

The measured SARs and radiation efficiencies are given in Table II ($d \approx 7$ mm). The corresponding simulation results with both heterogeneous and homogeneous head model are also given for comparison. With both head models, the trend in the SARs as a function of chassis length is the same, although homogeneous head models typically overestimate the local SAR values [25], [26], and thus higher SARs are obtained with the homogeneous than with the heterogeneous model, especially at 1800 MHz. Generally, the measured SARs are slightly lower than the simulated ones (homogeneous head model). The opposite differences in the maximum 10-g average SARs at 1800 MHz are assumed to be due to the different averaging schemes used in the simulations and measurements. However, it can be observed that the simulated and measured SAR values agree very well. Also the radiation efficiencies measured when the prototypes were positioned beside the head model follow well the simulated behavior.

As shown in Fig. 4, the general behavior of SARs and radiation efficiencies is rather similar with both distances between the head and phone. In general, the SARs in the head decrease and the radiation efficiency increases as the distance from the head to the chassis increases, as could be expected [10]. However, at 900 MHz the SARs are higher with $d \approx 7$ mm than with $d \approx 2$ mm when the chassis length is close to resonant. This is attributed to the decreased coupling to the chassis wavemode when there is lossy material (head) within a very short distance.

At 900 MHz, as the chassis length is increased with the phone very near the head ($d \approx 2$ mm), the SARs decrease with a slight local increase when the chassis is close to resonant length ($l_c \approx 0.36\lambda_0$). When the distance between the head and chassis is larger ($d \approx 7$ mm), the increase in SARs with the resonant chassis length is more clearly seen, and the global SAR maximums are obtained with resonant chassis. The highest radiation efficiencies are obtained with the shortest chassis lengths at both distances between the head and chassis. Thus, high local SARs do not necessarily mean low radiation efficiency, which is an exception to the general trend of the results. When increasing the chassis length, the radiation efficiency decreases significantly and reaches its minimum when the chassis is resonant. A further increase in the chassis length increases the radiation efficiency again. The differences between the maximum and minimum radiation efficiencies are roughly 2 and 3 dB for $d \approx 2$ mm and $d \approx 7$ mm, respectively.

At 1800 MHz, when the chassis length is increased, the SARs decrease fairly rapidly until the chassis reaches the first resonant length ($l_c \approx 0.36\lambda_0$). As the chassis length is increased from that, the SAR curves have a decreasing trend with local increases at higher order chassis resonances. The proximity of the head tunes the second chassis resonance down (from $l_c \approx 0.9\lambda_0$ to $l_c \approx 0.72\lambda_0$) compared to the free space situation. At 1800 MHz, the lowest radiation efficiencies are obtained with the smallest chassis lengths. As the chassis length is increased, the radiation efficiency increases slowly with local drops at chassis resonances. Regardless of the chassis length, the radiation efficiencies are roughly 1 dB higher with $d \approx 7$ mm compared to the values with $d \approx 2$ mm.

The distribution profiles illustrating the z-axis locations of the simulated maximum 10-g average SARs in the head are shown in Fig. 5 (see the coordinate system in Fig. 1). For all chassis lengths, the upper edge of the chassis was located at

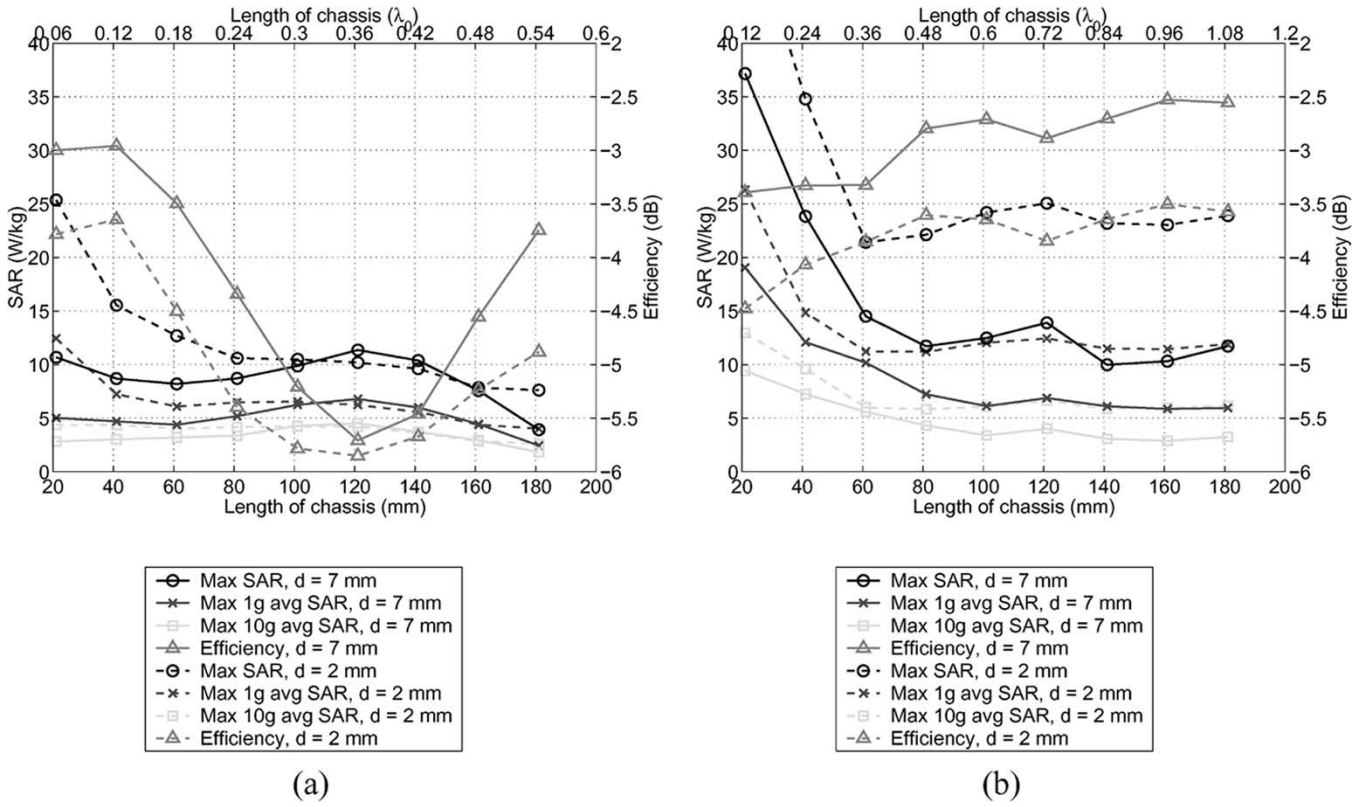

Fig. 4. SARs and radiation efficiencies as a function of chassis length at (a) 900 MHz and (b) 1800 MHz. Solid lines represent cases where distance from head to phone $d \approx 7$ mm. Dashed lines represent cases where $d \approx 2$ mm. $P_{\rm in} = 1$ W.

TABLE II
SIMULATED (SIM1: HETEROGENEOUS HEAD MODEL, SIM2: HOMOGENEOUS HEAD MODEL) AND MEASURED SARS AND RADIATION EFFICIENCIES BESIDE PHANTOM HEADS ($d \approx 7$ mm). $P_{\rm in} = 1$ W

	900 MHz								
Chassis length (mm)	**61**			**101**			**141**		
	Sim1	Sim2	Meas	Sim1	Sim2	Meas	Sim1	Sim2	Meas
Max *SAR* (W/kg)	8.2	8.9	8.3	9.9	10.1	9.8	10.4	9.8	8.8
Max 1g avg *SAR* (W/kg)	4.4	5.0	4.7	6.2	6.7	6.4	6.0	6.2	5.9
Max 10g avg *SAR* (W/kg)	3.2	3.3	3.0	4.3	4.5	4.4	3.7	4.3	3.6
η_r (dB)	-3.5	-3.4	-3.8	-5.2	-5.2	-5.0	-5.5	-5.4	-4.8
	1800 MHz								
Chassis length (mm)	**61**			**101**			**141**		
	Sim1	Sim2	Meas	Sim1	Sim2	Meas	Sim1	Sim2	Meas
Max *SAR* (W/kg)	14.5	21.1	19.8	12.5	16.8	15.5	10.0	13.4	12.7
Max 1g avg *SAR* (W/kg)	10.2	13.9	10.3	6.1	7.9	7.3	6.1	7.2	6.0
Max 10g avg *SAR* (W/kg)	5.6	6.3	6.2	3.4	3.7	4.0	3.1	3.4	3.8
η_r (dB)	-3.3	-3.3	-2.9	-2.7	-2.7	-2.6	-2.7	-2.7	-2.4

$z = 0$. For each chassis length, the maximum SAR value was recorded in each xy-plane, while the z-coordinate was increased from the lower edge of the chassis to 20 mm over the upper edge of the chassis. Thus, Fig. 5 gives no information on the depth (x) or sideward (y) locations of the SAR maximums. However, as is obvious, the SAR maximums are located near the head surface for all configurations. In the y-axis the locations fluctuate under the chassis area. Generally, the locations of the maximum unaveraged SARs, and maximum 1 g average SARs follow similar trends. Also the trends in the measured distributions are alike (Fig. 6).

At 900 MHz, the SAR maximums are generally located near the vertical center of the chassis, excluding the shortest chassis lengths $(l_c \leq 0.18\lambda_0)$, where the maximum SARs are located below the antenna element [Fig. 5(a)]. These results suggest that with $l_c > 0.18\lambda_0$ the antenna element does not have any significant effect on the SARs, but they are mainly caused by the dipole-type resonant mode of the chassis. Also, at 1800 MHz, the maximum SARs produced by the structures with the smallest chassis lengths $(l_c \leq 0.24\lambda_0)$ are located below the antenna element [Fig. 5(b)]. When the chassis length is close to the first resonant length $(l_c \approx 0.36\lambda_0)$, the SAR maximums are located near the vertically center part of the chassis. For $l_c > 0.48\lambda_0$, two local SAR maximums can be observed. The first maximum is located under the antenna element, and the second one lower in the chassis area, indicating that the chassis wavemode has a considerable contribution to the SARs also in these cases.

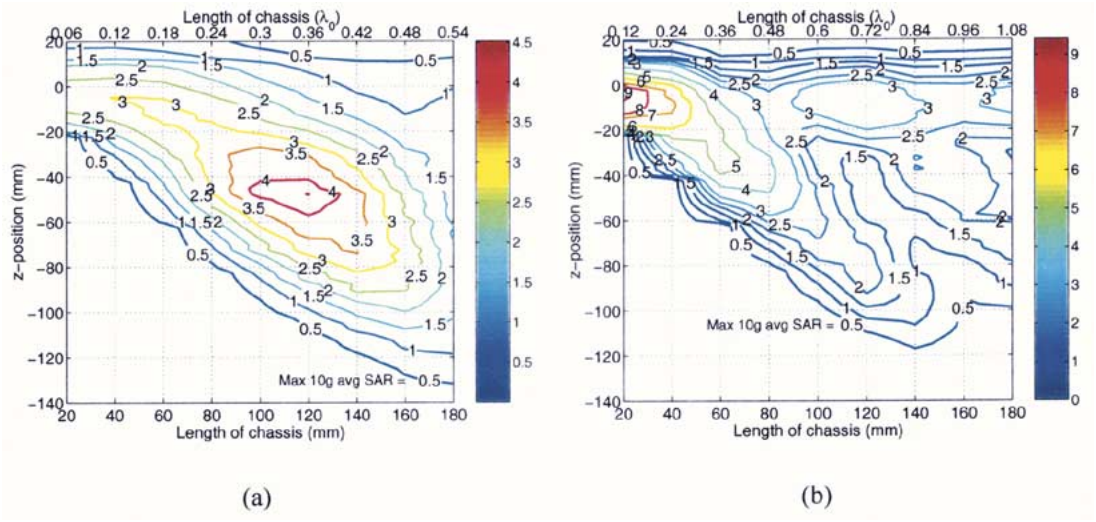

Fig. 5. Distribution profiles of maximum 10-g average SARs in watts per kilogram in head at (a) 900 MHz ($\mathrm{Max.} \approx 4.5$ W/kg) and (b) 1800 MHz ($\mathrm{Max.} \approx 9.4$ W/kg). Distance from head to phone $d \approx 7$ mm.

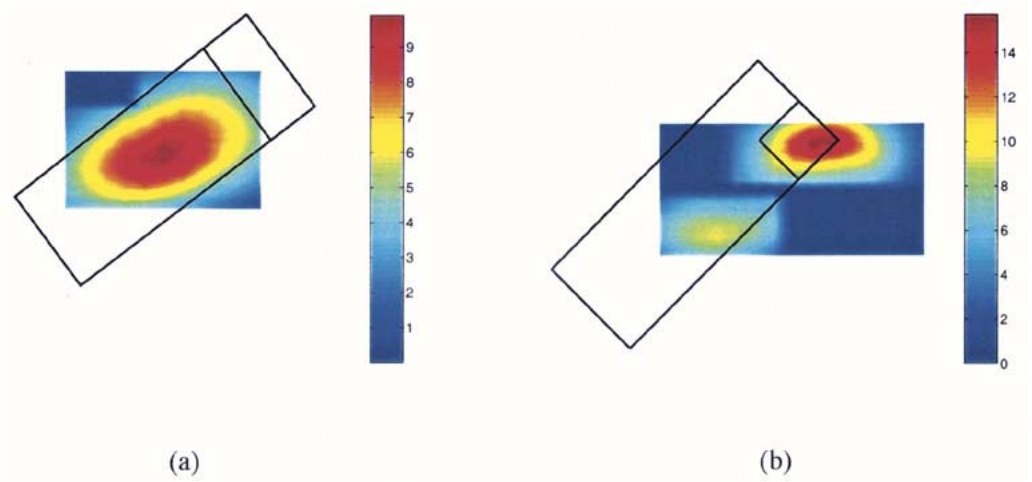

Fig. 6. Examples of the measured unaveraged SAR in watts per kilogram under the chassis area on the phantom surface at (a) 900 and (b) 1800 MHz. Chassis length $l_c = 101$ mm. Distance from head to phone $d \approx 7$ mm. $P_{\mathrm{in}} = 1$ W.

2) With Hand: The effect of the chassis length on the SARs and radiation efficiency was studied in the presence of the hand models as well ($d \approx 7$ mm). Similar general behavior in the SARs in the head was observed with either one of the hand models than without hand. Only the results with hand2 are illustrated with figures (Fig. 7). As expected [19], lower SARs in the head are obtained when a hand is present, because it absorbs some of the power. Owing to the shape and location of hand1 close to the chassis [see Fig. 2(a)], the SARs in the head are generally lower with hand1 than with hand2, and the average SARs in hand1 are higher than in hand2. The values of the 10-g average SARs in hand2 are very low and nearly constant with all chassis lengths (Fig. 7) due to their location in palm, which is relatively far from the chassis. The high unaveraged SARs in hand2 at 1800 MHz are explained by their location in the fingers near the chassis edge [see Fig. 2(b)].

Also, the trend in the radiation efficiency at 900 and at 1800 MHz, with either hand1 or hand2 included in the simulation, is rather similar to that obtained without hand. Compared to the radiation efficiencies without hand, at 900 MHz hand1 decreases the efficiency roughly by 2 to 4 dB when l_c is increased from 21 to 81 mm, and approximately 5 dB with longer chassis. The decrease due to hand2 is approximately 3 dB for $l_c < 61$ mm and approximately 4 dB otherwise. At 1800 MHz, the decreases due to hand1 and hand2 are approximately 3 and 2 dB, respectively.

C. Performance Comparison With Different Antenna Orientations

The effect of the antenna orientation with different chassis lengths was investigated by studying the performances of the antenna elements of Fig. 1 with different feed and short-circuit positions (Figs. 8–11). Locations marked with 1 (Loc1) are the configurations studied earlier in this section. The effect of different resonant frequencies caused by different feed and short-circuit positions and chassis lengths has not been removed from the results.

At 900 MHz, the impedance bandwidths (Fig. 8), as well as the SAR and radiation efficiency characteristics (see Figs. 4(a)

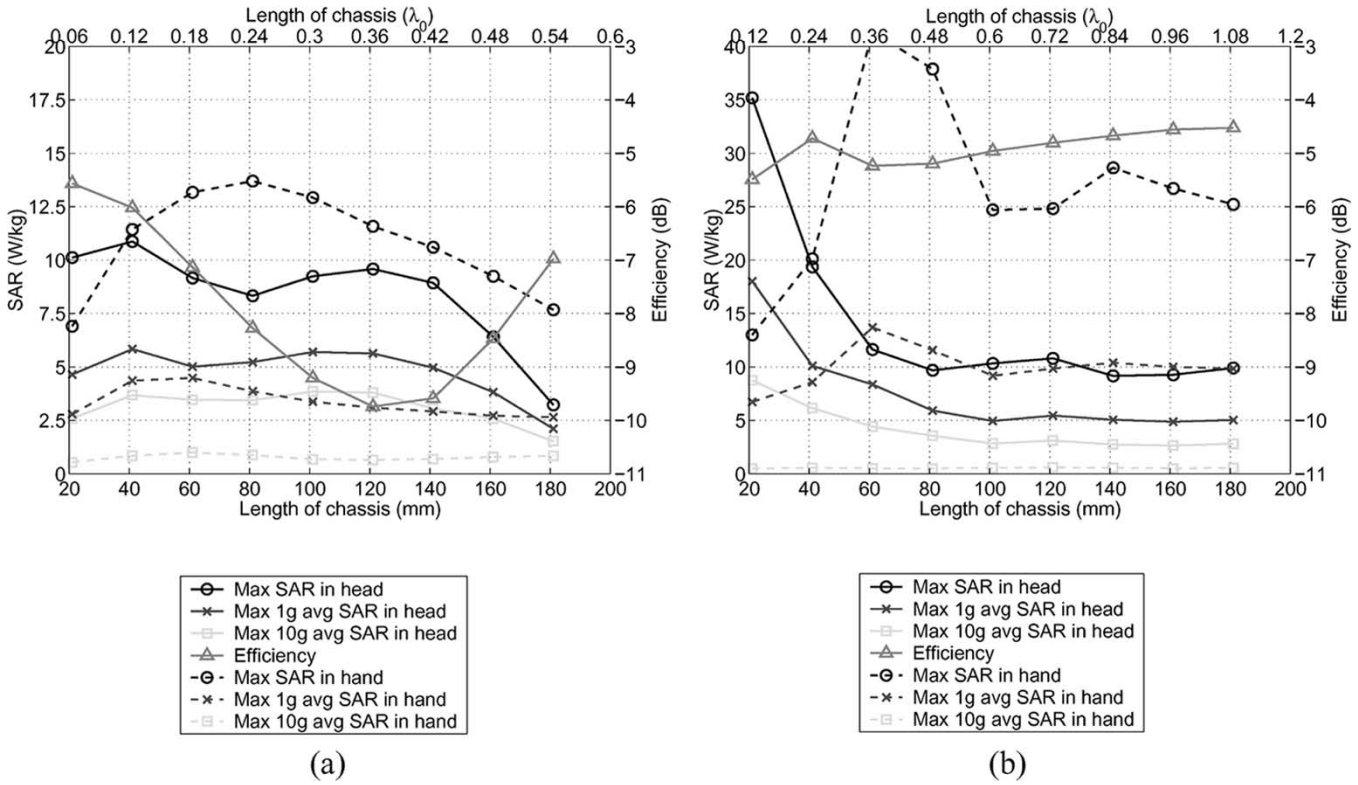

Fig. 7. SARs and radiation efficiencies as a function of chassis length with hand2 at (a) 900 and (b) 1800 MHz. Distance from head to phone $d \approx 7$ mm. $P_{\text{in}} = 1$ W.

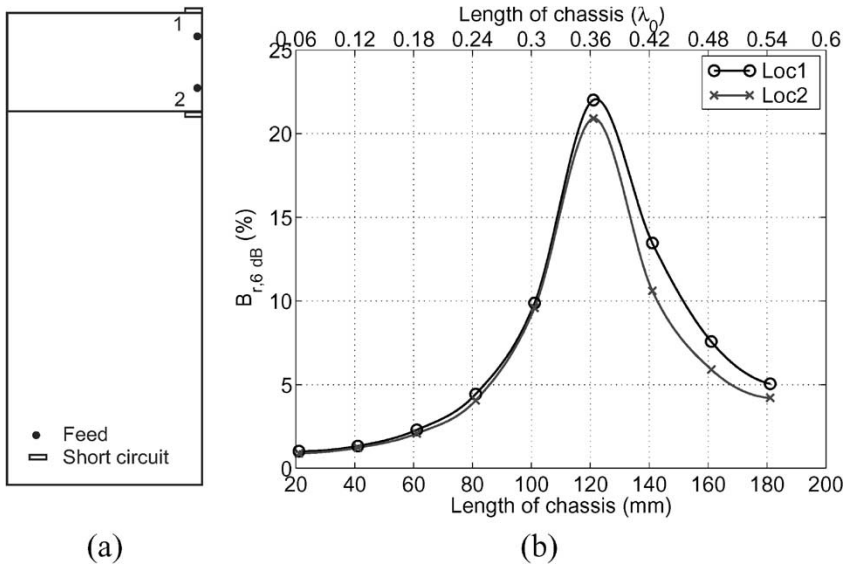

Fig. 8. (a) Antenna configurations for the 900-MHz model with different feed and short-circuit positions. Details of the antenna element are given in Fig. 1(a). (b) Simulated (MoM) impedance bandwidths ($L_{\text{retn}} \geq 6$ dB) in free space as a function of chassis length.

and 5(a) for Loc1), are quite similar with both antenna orientations. The reason for this is apparent; owing to the shape of the antenna element, there occur only relatively small changes in the current distribution of the antenna-chassis combination when turning the antenna element.

Fig. 9 shows that at 1800 MHz, larger bandwidth is obtained when the short circuit of the patch is located on the top of the chassis (Loc1 and Loc2) than in the opposite case where the radiating edge is located on the top (Loc3 and Loc4), which is expected [4], [27]. Although the bandwidth behavior of antennas with Loc1 and Loc2 is similar, the SAR features are not. Comparing Fig. 10(a) with Fig. 10(b), it is observed that the SARs are clearly lower with Loc2 than with Loc1. From the distribution profiles [Fig. 11(a) and (b)], it is seen that this is due to much lower SAR maximum near the antenna element with Loc2. The reason for this can be assumed to be the location of the loop formed by the feed and short circuit. For Loc1, this loop can excite currents flowing along the right edge of the chassis,

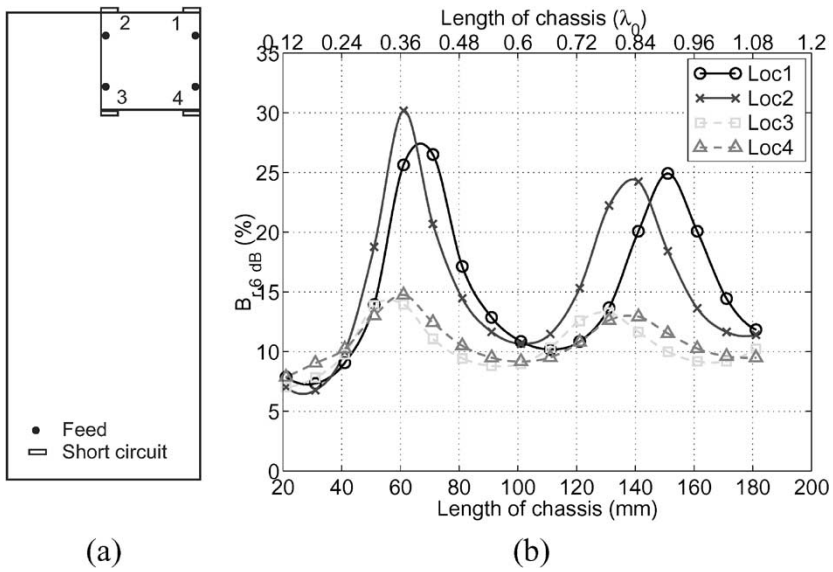

Fig. 9. a) Antenna configurations for the 1800-MHz model with different feed and short-circuit positions. Details of the antenna element are given in Fig. 1(b). (b) Simulated (MoM) impedance bandwidths ($L_{\rm retn} \geq 6$ dB) in free space as a function of chassis length.

but as in the case of Loc2 the respective loop is located perpendicularly to the top edge of the chassis, this is not possible. Basically, the SAR results with Loc3 follow those of Loc2 and the SAR results with Loc4 follow those of Loc1 (Figs. 10 and 11). It is worth noting that with $l_c = 0.36\lambda_0$, which gives the maximum bandwidth, the SARs are nearly equal, independent of the antenna orientation (Fig. 10). Thus, it can be expected that the antenna element wavemode has only a minor effect on the SARs in this case. It is also worth noting that lower in the chassis area ($z<-40$ mm) the SARs are similar in all four cases with all chassis lengths (Fig. 11). The radiation efficiency curves (Fig. 10) have similar drops in all four cases, when the chassis approaches the resonant length.

These results indicate that at 1800-MHz frequency range, it is possible to some extent optimize both bandwidth and SAR (or efficiency) by designing the antenna element so, that local SAR maximums are avoided. At 900 MHz, the chassis is the main source of radiation, and therefore, there does not seem to be many possibilities to affect the SAR obtained with a certain size of chassis.

V. Dependence of Antenna Performance on Other Chassis-Related Parameters

In this section, a systematic study on the effects of the chassis width and thickness on antenna performance is presented. Also, the effect of the distance between the head and chassis is studied with different chassis lengths. The two hand models of Section II-D are included in these studies as well. In addition, the effect of the position of the hand relative to the longitudinal axis of the chassis is investigated.

The antenna geometries and dimensions provided in Fig. 1 apply to all the studied structures of this section. Based on the good agreement between the computationally and experimentally obtained results in Section IV, the simulation models are considered valid, and this section is based on simulations only. For the limited space, all results cannot be illustrated with figures.

A. Chassis Width

The effect of the chassis width ($w_c = 3.6$–81 mm) on antenna performance was studied with two different chassis lengths, $l_c = 61$ mm and $l_c = 101$ mm, to get results for both longitudinally close to resonant and nonresonant chassis at both frequencies ($t_c = 3.6$ mm). The corner of the chassis, which was nearest to the short circuit of the antenna element, was fixed so that the antenna element was located in the corner of the chassis for all chassis widths (see Fig. 1). The chassis width was changed starting from a stick that was as wide as the short circuit (3.6 mm), thus, with the smallest chassis widths the antenna element was wider than the chassis. The distance between the head and chassis $d \approx 7$ mm.

The bandwidth values were calculated similarly as in the case of the chassis length. At both frequencies, the bandwidth increases clearly when the antenna element extends over the chassis edge, as the coupling between the antenna element and the chassis increases strongly [4]. Bandwidth values up to 60% are obtained, but in these cases the frequency response of the reflection coefficient is clearly dual-resonant, and the obtained bandwidth depends strongly on how well the dual-resonance is optimized. When the chassis is wider than the antenna element, the bandwidth remains roughly constant at 900 MHz ($B_{r,6\ \rm dB} \approx 2$–$3\%$ with $l_c = 61$ mm, $B_{r,6\ \rm dB} \approx 6\%$–$8\%$ with $l_c = 101$ mm). At 1800 MHz, the bandwidth increases when the chassis approaches the lateral resonance ($B_{r,\ 6\ \rm dB} \approx 19$–$24\%$ with $l_c = 61$ mm, $B_{r,\ 6\ \rm dB} \approx 13$–$32\%$ with $l_c = 101$ mm).

At both frequencies, when the width of the chassis is narrower than that of the antenna element, and the bandwidth is increased due to the large contribution of the chassis wavemode, the SARs increase and the radiation efficiencies decrease strongly (see

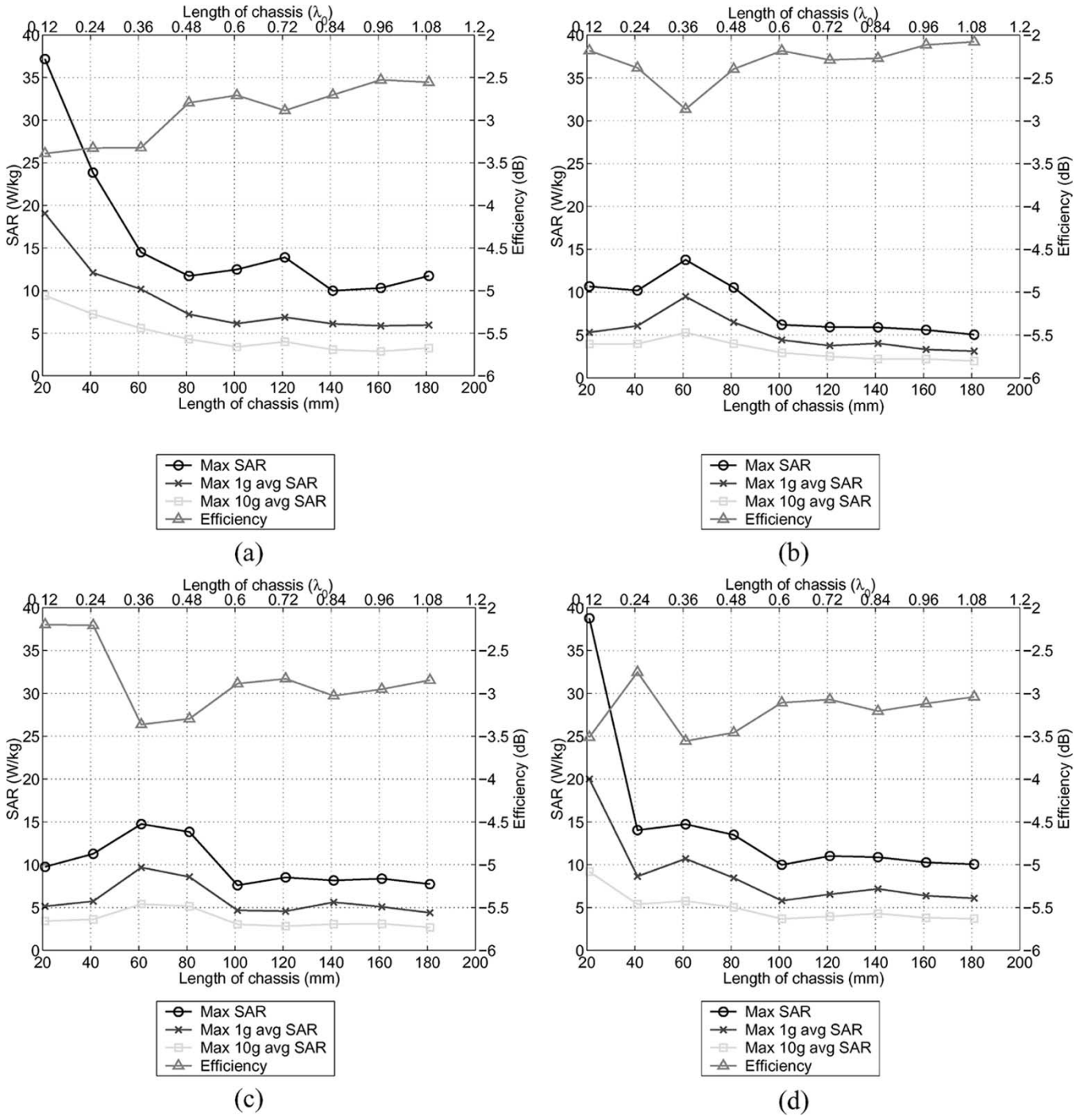

Fig. 10. SARs and radiation efficiencies as a function of chassis length at 1800 MHz. (a) Loc1. (b) Loc2. (c) Loc3. (d) Loc4. Distance from head to phone $d \approx 7$ mm. $P_{\text{in}} = 1$ W.

Fig. 12). Then, the SAR maximums are located near the vertically center part of the chassis with the chassis near the resonant lengths, and their values are higher than those with the nonresonant chassis lengths. For $w_c \leq 41$ mm with the nonresonant chassis lengths and for $w_c > 41$ mm, the antenna element contributes more to the SARs, and the maximums are generally located close to the antenna element. An exception is the case with the chassis near the lateral resonance at 1800 MHz ($w_c \approx$ 50–60 mm), when the maximum SARs are located in the laterally center part of the chassis. The radiation efficiencies are lower with the chassis near the resonant lengths than with the nonresonant chassis lengths; for $w_c \leq 41$ mm, the difference is approximately 2 dB at 900 MHz and approximately 1 dB at 1800 MHz. With wider chassis, the differences get smaller at both frequencies.

The effect of the chassis width ($l_c = 101$ mm, $t_c = 3.6$ mm) was studied also in the presence of hand models. For $w_c =$ 3.6–41 mm, the hands were modeled as in Fig. 2, and the narrow chassis were located just beside the fingers. For $w_c > 41$ mm, the palm (y dimension) was also widened as a function of w_c,

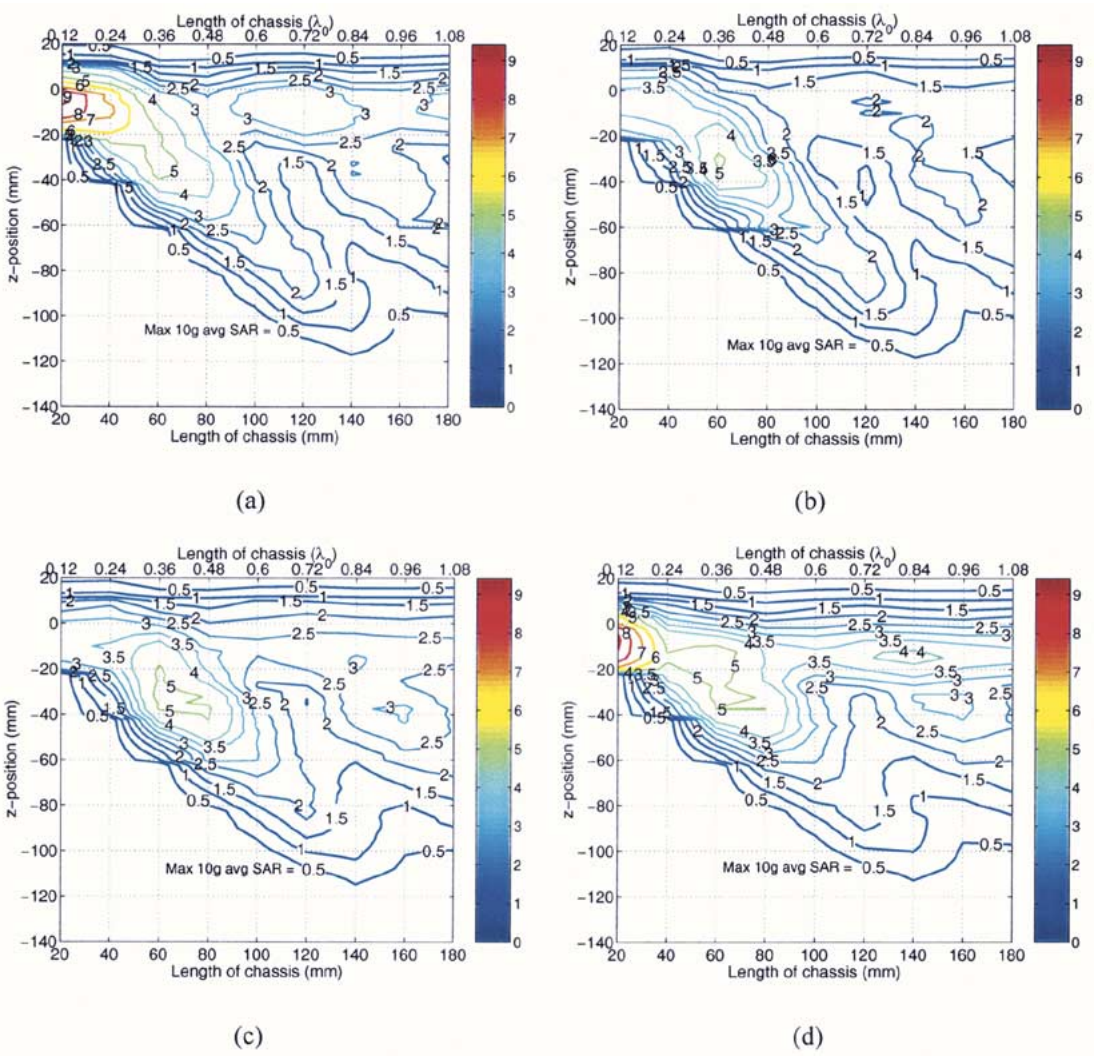

Fig. 11. Distribution profiles of maximum 10-g average SARs in watts per kilogram in head at 1800 MHz.(a) Loc1 ($\mathrm{Max.} \approx 9.4\ \mathrm{W/kg}$). (b) Loc2 ($\mathrm{Max.} \approx 5.3\ \mathrm{W/kg}$). (c) Loc3 ($\mathrm{Max.} \approx 5.4\ \mathrm{W/kg}$). (d) Loc4 ($\mathrm{Max.} \approx 9.2\ \mathrm{W/kg}$).

so that the fingers wrapped the chassis similarly with all chassis widths.

At 900 and 1800 MHz, when $w_c \geq 41$ mm, the general trends in the SARs in the head and in the radiation efficiencies, with either hand1 or hand2 included in the model, are similar to those obtained without hand (Fig. 12), including also the locations of the SAR maximums. With a very narrow chassis at 1800 MHz ($w_c < 41$ mm), most of the power is absorbed by the hands, and the SARs in the head are nearly constant and clearly lower than those without hand: the SARs obtained with hand1 and hand2 are approximately 20%–60% and 40%–75% of those without hand, respectively. The SARs in the hands follow basically the same behavior as the SARs in the head, although the values are higher than those in the head. At 900 MHz, the difference in the radiation efficiency without hand and with hand1 is roughly 5 dB with all chassis widths. The decrease in the radiation efficiency owing to hand2 is roughly from 2 to 4 dB when w_c increases from 3.6 to 41 mm and roughly 5 dB with wider chassis widths. At 1800 MHz, the decrease due to hand1 is approximately 4 dB for $w_c < 41$ mm and 3 dB otherwise, and the decrease due to hand2 is 3 and 2 dB, respectively.

B. Chassis Thickness

The effect of the chassis thickness ($t_c = 1.1$–11.1 mm) was studied with the chassis of $l_c = 101$ mm and $w_c = 41$ mm. The distance between the head and chassis was kept constant in all cases ($d \approx 7$ mm), thus also the distance between the head and antenna element increased as a function of chassis thickness.

The chassis thickness has only a minor effect on the impedance bandwidth (one percent unit at maximum) at both frequencies. The general trends in the SARs and radiation efficiency are similar to those caused by changing the distance between the head and chassis: due to the weaker near fields the SARs in the head decrease and the radiation efficiencies increase as the chassis thickness is increased (see Section V-C). Thus, it is important to use a realistic chassis thickness, which is typically a few millimeters in today's handsets, as the SAR and efficiency results for thicker chassis often used in the literature (roughly 20 mm) are quite different from those for the typical modern handset. Also, it is interesting to notice that both at 900 and 1800 MHz, the SARs and radiation efficiencies at equal distances between the head and antenna element, and

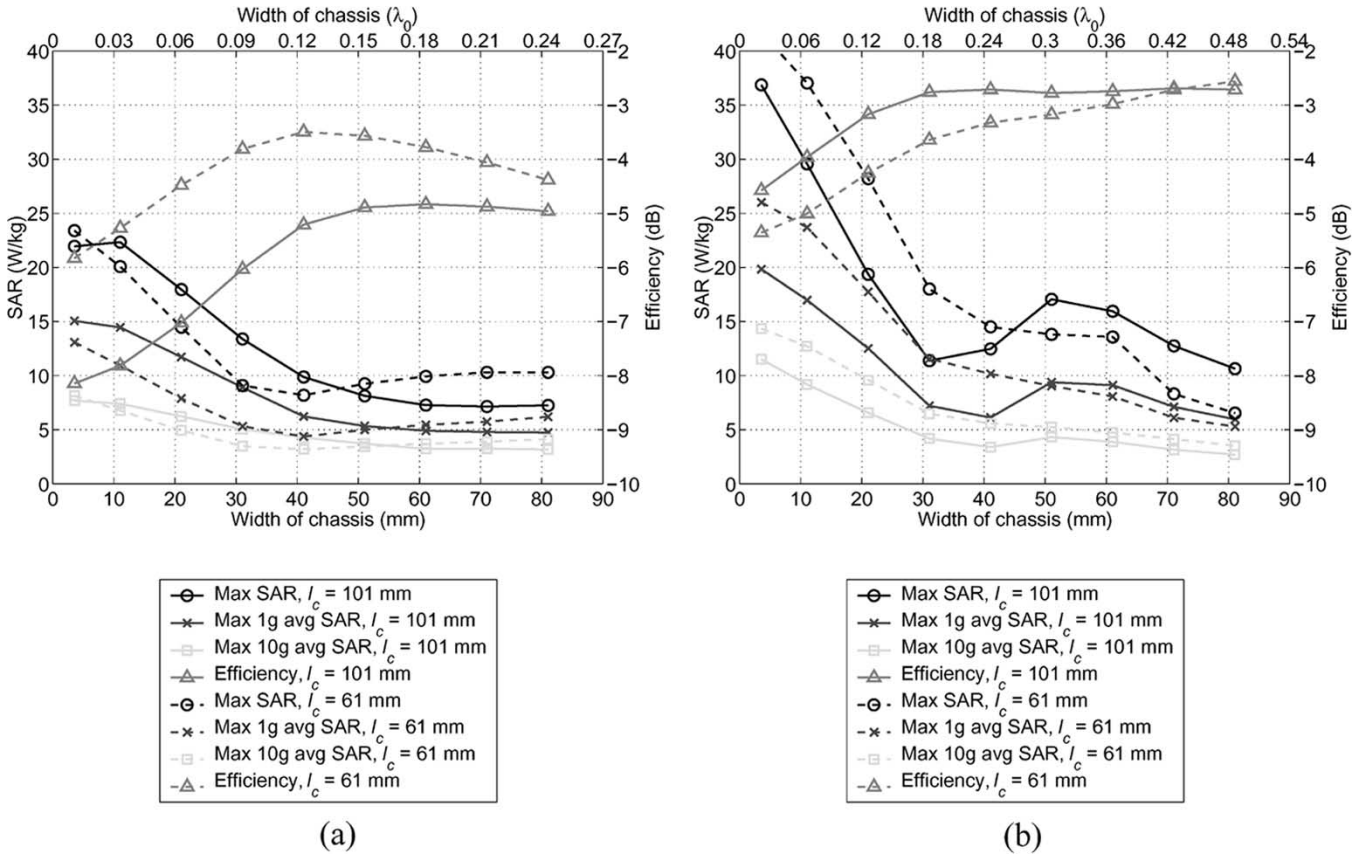

Fig. 12. SARs and radiation efficiencies as a function of chassis width with two chassis lengths ($l_c = 101$ mm and $l_c = 61$ mm) at (a) 900 and (b) 1800 MHz. Distance from head to phone $d \approx 7$ mm. $P_{\text{in}} = 1$ W.

thus equal distances between the head and front side of the chassis, are roughly equal regardless of the chassis thickness.

C. Distance Between the Head and Phone

The effect of the distance between the head and phone chassis ($d \approx 0$–14.5 mm) on the SARs and radiation efficiency was studied with two different chassis lengths, $l_c = 61$ mm and $l_c = 101$ mm, which were selected based on the chassis resonances ($w_c = 41$ mm, $t_c = 3.6$ mm).

Predictably [10], the SARs decrease and the radiation efficiencies increase as the distance from the head to chassis increases (Fig. 13). However, the results of Fig. 13 give novel information, as it is noted that when the chassis is close to resonant, the SARs decrease slower as a function of distance than when the chassis is nonresonant. An exception to the trend is the situation when the metal chassis touches the head, in which case the SARs are roughly equal with both chassis lengths. The radiation efficiencies are roughly 1.5 dB lower at 900 MHz and 0.5 dB lower at 1800 MHz with chassis close to resonant lengths than with nonresonant chassis lengths, excluding the case when the chassis touches the head.

When the effect of distance was studied with hand models, the location of the hand was fixed with respect to the chassis (see Fig. 2), i.e., the hand was also moved as a function of distance between the head and phone. Generally, with either one of the hand models, the behavior of the SARs in the head is similar to the case without hand (Fig. 13). The farther the chassis and hand are from the head, the more the SARs in the head are reduced compared to the values without hand. However, the SARs in hands increase at the same time. At 900 MHz, when the distance increases from 2 to 14.5 mm, the SARs in the head with hand1 are approximately 70%–60% and with hand2 90%–80% of those without hand. Correspondingly, at 1800 MHz the SARs in the head with hand1 are approximately 95%–50%, and with hand2 90%–70% of the values without hand. Hand1 reduces the radiation efficiency the most with the largest distances; the decrease is roughly 4–6 dB at 900 MHz and 2–3 dB at 1800 MHz when $d = 2$–14.5 mm. The decrease due to hand2 is roughly 4 dB at 900 MHz and 2 dB at 1800 MHz.

D. Hand Position

The effect of the hand position relative to the longitudinal axis of the chassis on the SARs and radiation efficiency was studied for both hand models with $l_c = 121$ mm ($w_c = 41$ mm, $t_c = 3.6$ mm). With that length, the contribution of the chassis wavemode is at its maximum at 900 and at its minimum at 1800 MHz (see Fig. 3). Only the results with hand2 are illustrated with figures. In Fig. 14, "0 mm" denotes the location of the upper edge of the hand in the plane of the upper edge of the phone chassis, and "120 mm" denotes the location of the upper edge of the hand in the plane of the lower edge of the chassis, i.e., the hand has slipped off the chassis.

With both hand models at 900 MHz, the hand position has only a minor effect on the SARs in the head. Generally, the SARs in both hands decrease and the radiation efficiency increases slowly as the hand moves farther away from the antenna

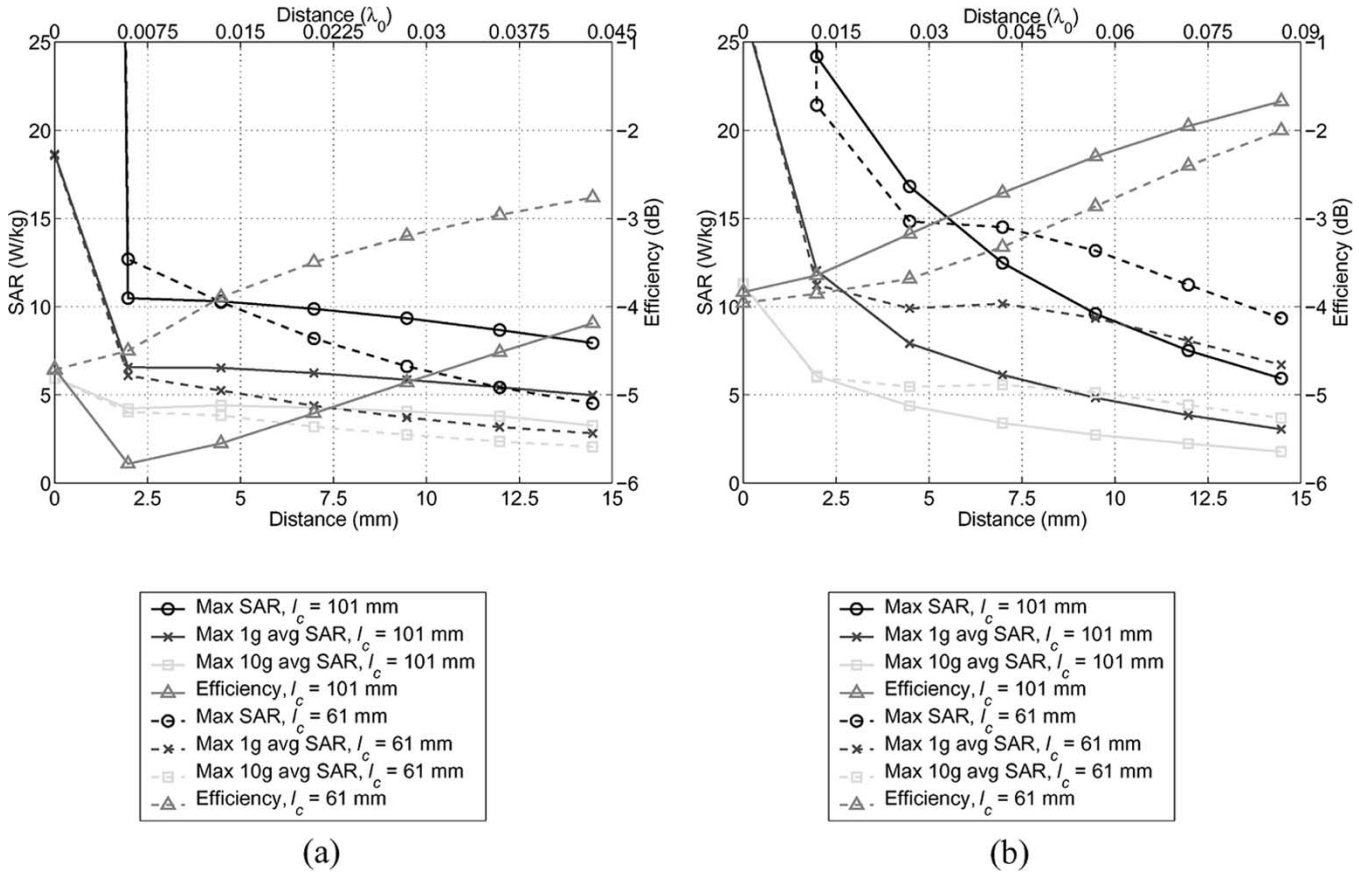

Fig. 13. SARs and radiation efficiencies as a function of the distance between head and phone with two chassis lengths ($l_c = 101$ mm and $l_c = 61$ mm) at (a) 900 and (b) 1800 MHz. $P_{\rm in} = 1$ W.

element. Fig. 14(a) shows an interesting result: when hand2 is moved from the top of the antenna element just below it (from "0 mm" to "20 mm"), the radiation efficiency in fact decreases by 1.5 dB. This is assumed to be the case because in this case (at 900 MHz with $l_c = 121$ mm), the chassis is actually the main radiator, and the effect of the hand is larger when it covers the vertically center part of the chassis than when it covers the antenna element. At 1800 MHz, the SARs in the head increase slowly as the hand is moved farther away from the antenna element, and the SARs in both hand models decrease. The radiation efficiencies with both hand models increase rapidly, roughly by 6 dB, until the upper edge of the hand is 20 mm below the antenna element (hand position "40 mm"), but then the values are nearly constant (around -3 dB with hand1 and -4 dB with hand2).

The different behaviors of hand positions at 900 and 1800 MHz with a 121-mm-long chassis support the results that at 900 MHz, the chassis is resonant and thus the main radiator, and that at 1800 MHz, the contribution of the antenna element wavemode is larger. Therefore, the hand location has a significant effect on the radiation efficiency at 900 MHz, but at 1800 MHz the radiation efficiency does not change much when the hand is located further away from the antenna element.

VI. Discussion

One important but often less considered factor of handset antenna design is the chassis on which the antenna element is mounted. The results of this paper indicate clearly that the bandwidth, efficiency, and SAR characteristics of mobile phone antennas are strongly affected by the chassis. The significance of the chassis length on handset antenna performance was studied first. It was shown that the impedance bandwidth of the studied combinations of antenna and phone chassis depends strongly on the effective length of the chassis ($l_{c,\rm eff}$), with the maximums obtained when $l_{c,\rm eff}$ is a multiple of approximately $0.5\lambda_0$ at the operating frequency ($l_{c,\rm eff} \approx 0.5\lambda_0$ corresponds to the physical chassis length $l_c \approx 0.4\lambda_0$). Thus, from the bandwidth point of view, the ideal case is when the resonant frequency of the chassis is close to that of the antenna element [4]. However, it was noted that when the thick dipole-type chassis is at resonance and the obtained bandwidth reaches its maximum, an increase in SARs and a decrease in radiation efficiency occur compared to the general trend. As an example, the performance of the studied antenna elements on 61- and 121-mm-long chassis ($w_c = 41$ mm, $t_c = 3.6$ mm) is compared based on Figs. 3 and 4 ($d \approx 7$ mm). These two chassis lengths were selected due to the chassis resonances. The point $l_c = 61$ mm is near a bandwidth minimum at 900 MHz, suggesting that the chassis is nonresonant, and near a bandwidth maximum at 1800 MHz, suggesting that the chassis is resonant. The situation is just the opposite when $l_c = 121$ mm. At 900 MHz, when the chassis length is changed from 61 to 121 mm (from $0.18\lambda_0$ to $0.36\lambda_0$), the impedance bandwidth increases by a factor of 11, the average SARs in the head increase by a factor of 1.5, whereas the

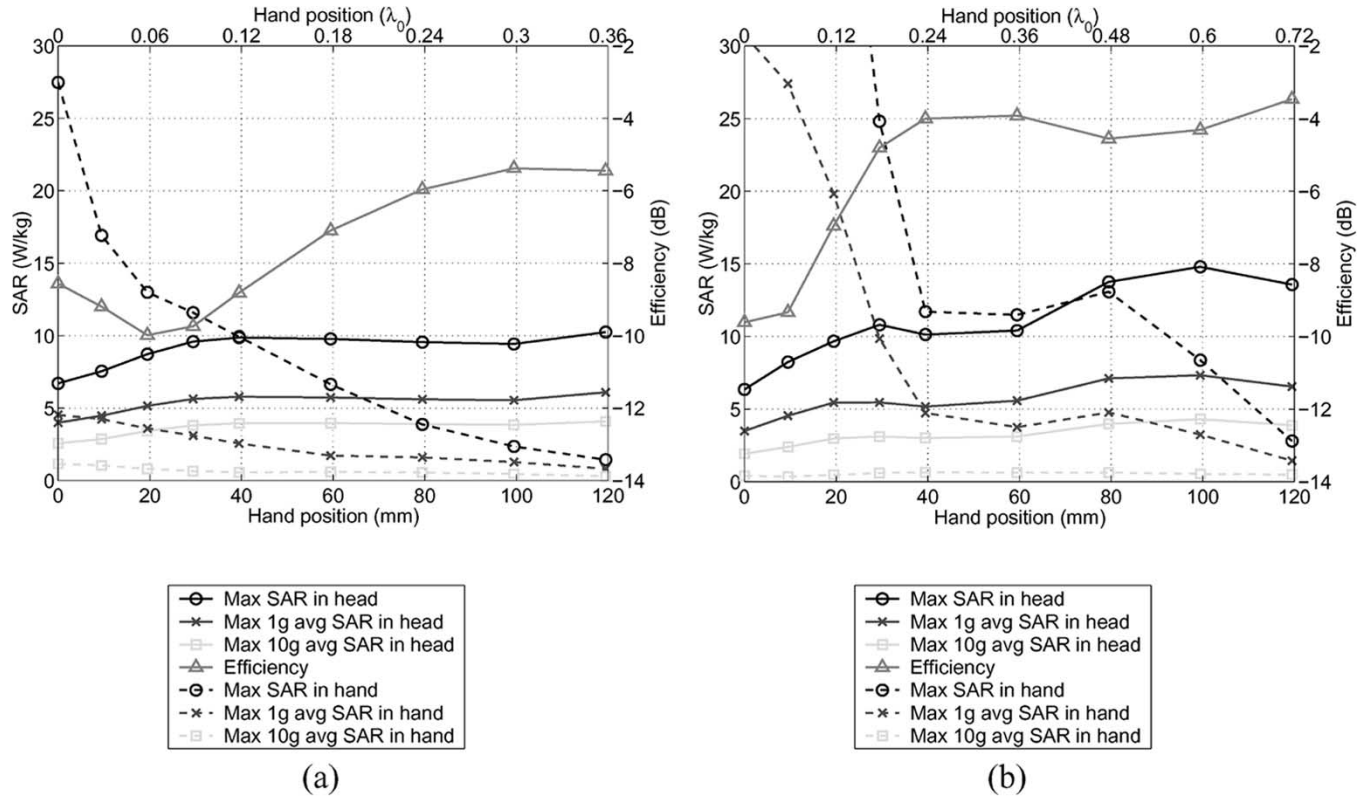

Fig. 14. SARs and radiation efficiencies as a function of hand2 position (0 mm = upper edge of the phone chassis, 120 mm = lower edge of the phone chassis) at (a) 900 and (b) 1800 MHz. Chassis length $l_c = 121$ mm. Distance from head to phone $d \approx 7$ mm. $P_{\text{in}} = 1$ W.

radiation efficiency decreases by 2.2 dB. Correspondingly, at 1800 MHz, the impedance bandwidth is halved when the chassis length is changed from 61 to 121 mm (from $0.36\lambda_0$ to $0.72\lambda_0$). At the same time the average SARs in the head decrease approximately by a factor of 1.5, and the radiation efficiency improves slightly (≈ 0.4 dB).

Hence, there seems to be an obvious connection between the impedance bandwidths, SARs, and radiation efficiencies: higher SAR values and lower radiation efficiency are obtained in cases where the bandwidth increases due to the strong excitation of the chassis wavemode. The contribution of the chassis wavemode is dominant when the chassis is resonant and emphasized at lower frequencies. Also, the presented SAR distribution profiles support these findings. To confirm the analysis, the effect of several other chassis-related parameters—width, thickness, and distance between the head and phone—on handset antenna performance was studied. Also, all these results support the conclusions made above. Besides, the results obtained in this paper are fully consistent with the results of [4], [5], where it was shown that for moderate bandwidths ($\approx 10\%$) the radiation of the small antenna element of a typical mobile handset at 900 MHz represents only a small portion ($\approx 10\%$) of the total radiated power, and that at 1800 MHz the antenna element is more significant ($\approx 50\%$). In addition, further studies of the SAR and efficiency features of the internal multiband mobile phone antenna presented in [13] show that the presented characteristics could be applied to dualband or multiband antenna elements as well, and scaled to other frequency ranges, even though the study of this paper is realized for 900 MHz and 1800 MHz antenna elements separately. Thus, the results of this paper are considered to represent the typical characteristics of internal mobile phone antennas and can be generalized to apply to any similar patch-type antenna elements. Moreover, based on [4], the type of the antenna—whether it is internal or external—is not significant for the SAR or efficiency at 900 MHz, where the chassis wavemode typically dominates.

As the antenna elements used in the study represent typical internal mobile phone antennas concerning the impedance bandwidth, the electrical volume of the 1800 MHz element is four times that of the 900 MHz element. Based on [4], it is assumed that this is the main reason why the changes in various characteristics caused by the chassis resonances are relatively smaller for the 1800-MHz element. Decreasing the electrical size of the 1800-MHz element should bring the results closer to those of the 900-MHz element, assuming that the bandwidth is kept constant, which requires increasing the coupling between the antenna element and chassis wavemodes.

Also the chassis models used in this study were selected realistic; chassis dimensions and distances represent the typical values of modern mobile handsets. The SAR values in the head obtained with these models are in many cases around the specified maximum values 1.6 W/kg averaged over 1 g of tissue [28] and 2.0 W/kg averaged over 10 g of tissue [18]. Thus, it is obvious that attention has to be paid to the chassis design not to exceed the specified limits. Although the measured SARs agree well with the simulated values, it is still not reasonable to draw any further conclusions about the absolute SAR values of this paper compared to those of commercial mobile phones owing to

several differences between the studied prototypes and commercial products. However, values of the same order as in this paper have been presented in [6] for similar prototype structures. This study also demonstrates that the worst case SAR values in the head are obtained without hand. The SAR values in the hand models used in this work are clearly lower than the specified maximum value 4.0 W/kg averaged over 10 g of tissue [18], [28]. However, the study shows that concerning the efficiency of the antenna-chassis combination, it is necessary to consider also the effect of the hand, as the decrease in efficiency due to the hand may be several decibels depending on the configuration.

The presented results also indicate that the type of the used phantom is of major importance when considering the SAR characteristics. The results seem not to be very sensitive to the differences in anatomical head model type, as simulations with the specific anthropomorphic mannequin (SAM) head give similar results to those presented in this paper. However, the shape of the phantom is significant, as it was noted that the results are not consistent with those obtained when using nonanatomical, simplified phantoms (sphere, cube) [8], [11]. At 900 MHz, instead of a maximum, a SAR minimum was reached at the chassis resonance with the maximum bandwidth when using a flat phantom [11]. At 1800 MHz, the maximum SARs increased as a function of chassis length [11], whereas in this paper just the opposite trend was found. The behavior of radiation efficiency as a function of chassis parameters was not reported in [8], [11]. A study on the radiation efficiency characteristics of the antenna structures of this paper beside a homogeneous cubic head model, which is similar to that used in [11], shows that at chassis resonances there are similar drops in the radiation efficiency as beside an anatomical head model.

VII. Conclusion

This paper has presented one key issue relating to the design of internal mobile phone antennas. In the paper, the effects of several chassis-related parameters—length, width, thickness, and the distance from head to phone—on the bandwidth, radiation efficiency, and specific absorption rate characteristics of microstrip-type handset antennas were analyzed. The antenna-chassis combinations were in actual handset use position beside an anatomical head model. The study also contained two different hand models.

The presented analysis increases the understanding of the combined behavior of antenna and chassis and provides novel and useful information for future design of mobile handset antennas. The results show the general trends of bandwidth, SAR, and efficiency with different chassis parameters. The results lead to the conclusion that the conventional antenna element-based approach is not adequate for objective evaluation of the performance of mobile phone antennas, but the effect of the mobile chassis should always be included in all considerations of bandwidth, efficiency, or SAR characteristics. The results also show that with the used models there is a clear connection between the general behavior of impedance bandwidth, SARs, and radiation efficiency. In general, when the bandwidth reaches its maximum due to the increased contribution of a resonant chassis, an increase in SARs and a decrease in radiation efficiency occur compared to the general trend. Thus, it can be concluded that when reporting any SAR or efficiency values of mobile phone antennas, it is essential to give information also on the impedance bandwidth.

Acknowledgment

The authors wish to thank Dr. C. Icheln for his help in the radiation efficiency measurements and for his kind assistance with the simulators.

References

[1] T. Taga and K. Tsunekawa, "Performance analysis of a built-in planar inverted F antenna for 800 MHz band portable radio units," *IEEE J. Select. Areas Commun.*, vol. SAC-5, pp. 921–929, June 1987.

[2] K. Sato, K. Matsumoto, K. Fujimoto, and K. Hirasawa, "Characteristics of a planar inverted-F antenna on a rectangular conducting body," *Electron. Commun. Japan*, pt. 1, vol. 72, pp. 43–51, 1989.

[3] T. Taga, "Analysis of planar inverted-F antennas and antenna design for portable radio equipment," in *Analysis, Design, and Measurement of Small and Low-Profile Antennas*, K. Hirasawa and M. Haneishi, Eds. Norwood, MA: Artech House, 1992, pp. 161–180.

[4] P. Vainikainen, J. Ollikainen, O. Kivekäs, and I. Kelander, "Resonator-based analysis of the combination of mobile handset antenna and chassis," *IEEE Trans. Antennas Propagat.*, vol. 50, pp. 1433–1444, Oct. 2002.

[5] ——, "Performance analysis of small antennas mounted on mobile handset," in *Proc. COST 259 Final Workshop—Mobile Terminal and Human Interaction*, 2000, p. 8.

[6] D. Manteuffel, A. Bahr, and I. Wolff, "Investigation on integrated antennas for GSM mobile phones," in *Proc. Millennium Conf. Antennas Propagat.*, 2000, paper p0351.pdf.

[7] D. Manteuffel, A. Bahr, D. Heberling, and I. Wolff, "Design considerations for integrated mobile phone antennas," in *Proc. 11th Int. Conf. Antennas Propagat.*, 2001, pp. 252–256.

[8] A. T. Arkko and E. A. Lehtola, "Simulated impedance bandwidths, gains, radiation patterns and SAR values of a helical and a PIFA antenna on top of different ground planes," in *Proc. 11th Int. Conf. Antennas Propagat.*, 2001, pp. 651–654.

[9] N. Kuster and Q. Balzano, "Energy absorption mechanism by biological bodies in the near field of dipole antennas above 300 MHz," *IEEE Trans. Veh. Technol.*, vol. 41, pp. 17–23, Feb. 1992.

[10] M. A. Jensen and Y. Rahmat-Samii, "EM interaction of handset antennas and a human in personal communications," *Proc. IEEE*, vol. 83, pp. 7–17, Jan. 1995.

[11] D. Manteuffel, A. Bahr, P. Waldow, and I. Wolff, "Numerical analysis of absorption mechanisms for mobile phones with integrated multiband antennas," in *Proc. IEEE Antennas Propagation Symp.*, 2001, pp. 82–85.

[12] R. J. Luebbers and H. S. Langdon, "A simple feed model that reduces time steps needed for FDTD antenna and microstrip calculations," *IEEE Trans. Antennas Propagat.*, vol. 44, pp. 1000–1005, July 1996.

[13] J. Ollikainen, O. Kivekäs, A. Toropainen, and P. Vainikainen, "Internal dual-band patch antenna for mobile phones," in *Proc. Millennium Conf. Antennas Propagat.*, 2000, paper p1111.pdf.

[14] G. Waldschmidt and A. Taflove, "The determination of the effective radius of a filamentary source in the FDTD mesh," *IEEE Microwave Guided Wave Lett.*, vol. 10, pp. 217–219, June 2000.

[15] *User's Manual for XFDTD the Finite Difference Time Domain Graphical User Interface for Electromagnetic Calculations, Version 5.04*, Remcom, State College, PA, 1999.

[16] H. Q. Woodard and D. R. White, "The composition of body tissues," *British J. Radiol.*, vol. 59, pp. 1209–1219, Dec. 1986.

[17] D. R. White, H. Q. Woodard, and S. M. Hammond, "Average soft-tissue and bone models for use in radiation dosimetry," *British J. Radiol.*, vol. 60, pp. 907–913, Sept. 1987.

[18] "European Specification (ES 59 005) Considerations for the evaluation of human exposure to electromagnetic fields (EMFs) From mobile telecommunication equipment (MTE) in the frequency range 30 MHz–6 GHz," CENELEC, Brussels, Belgium, 1998.

[19] J. T. Rowley and R. B. Waterhouse, "Performance of shorted microstrip patch antennas for mobile communications handsets at 1800 MHz," *IEEE Trans. Antennas Propagat.*, vol. 47, pp. 815–822, May 1999.

[20] "Recipes for brain tissue simulating liquids," Schmid & Partner Engineering AG, Zurich, Switzerland, 1999.
[21] Q. Yu, O. P. Gandhi, M. Aronsson, and D. Wu, "An automated SAR measurement system for compliance testing of personal wireless devices," *IEEE Trans. Electromagn. Compat.*, vol. 41, pp. 234–245, Aug. 1999.
[22] H. Arai, *Measurement of Mobile Antenna Systems*. Boston, MA: Artech House, 2001, pp. 56–57.
[23] A. G. Derneryd, "The circular microstrip antenna element," in *Proc. Int. Conf. Antennas Propagation*, 1978, pp. 307–311.
[24] R. E. Collin, *Antennas and Radiowave Propagation*. Singapore: McGraw-Hill, 1985, pp. 35–38.
[25] V. Hombach, K. Meier, M. Burkhardt, E. Kühn, and N. Kuster, "The dependence of EM energy absorption upon human head modeling at 900 MHz," *IEEE Trans. Microwave Theory Tech.*, vol. 44, pp. 1865–1873, Oct. 1996.
[26] K. Meier, V. Hombach, R. Kästle, R. Y.-S. Tay, and N. Kuster, "The dependence of electromagnetic energy absorption upon human-head modeling at 1800 MHz," *IEEE Trans. Microwave Theory Tech.*, vol. 45, pp. 2058–2062, Nov. 1997.
[27] M. Geissler, D. Heberling, and I. Wolff, "Properties of integrated handset antennas," in *Proc. Millennium Conf. Antennas Propagation*, 2000, paper p0526.pdf.
[28] *IEEE Standard for Safety Levels With Respect to Human Exposure to Radio Frequency Electromagnetic Fields 3 kHz to 300 GHz*, ANSI/IEEE Standard C95.1, 1999.

Outi Kivekäs was born in Helsinki, Finland, in 1974. She received the Master of Science in Technology and Licentiate of Science in Technology degrees in electrical engineering in 1999 and 2001, respectively, from Helsinki University of Technology (HUT), Helsinki, Finland, where she is currently working toward the doctorate degree.

Since 1998, she has been a Research Engineer at the Radio Laboratory, HUT. Her research interests include mobile terminal antennas and their user interaction.

Jani Ollikainen (M'03) was born in Lahti, Finland, in 1971. He received the Master of Science and Licentiate of Technology degrees in electrical engineering in 1997 and 2000, respectively,from Helsinki University of Technology (HUT), Helsinki, Finland, where he is currently working to complete the Doctor of Science degree.

From 1996 until 2003, he worked as a Researcher at the Radio Laboratory of HUT. In early 2003, he joined Nokia Research Center, Helsinki, Finland, where he is currently working as a Senior Research Engineer. His research interests include design, implementation, and measurement techniques of small antennas for personal mobile communications.

Tuukka Lehtiniemi was born in Helsinki, Finland in 1980. He is currently working toward the Master of Science degree in electrical engineering at Helsinki University of Technology (HUT), Helsinki, Finland.

He works as a trainee at the Radio Laboratory, HUT.

Pertti Vainikainen (M'91) was born in Helsinki, Finland in 1957. He received the Master of Science in Technology, Licentiate of Science in Technology, and Doctor of Science in Technology degrees from Helsinki University of Technology (HUT) in 1982, 1989 and 1991, respectively.

From 1992 to 1993 he was Acting Professor of Radio Engineering, since 1993, an Associate Professor of Radio Engineering, and since 1998, Professor in Radio Engineering, all at the Radio Laboratory of HUT. From 1993 to 1997, he was the Director of the Institute of Radio Communications (IRC) of HUT, and in 2000, a Visiting Professor at Aalborg University, Aalborg,Denmark. His main fields of interest are antennas and propagation in radio communications and industrial measurement applications of radio waves. He is the author or coauthor of three books, about 170 refereed international journal or conference publications, and the holder of six patents.